J Nanopart Res (2013) 15:1527
DOI 10.1007/s11051-013-1527-3

RESEARCH PAPER

Measuring Friedel pairs in nanomembranes of GaAs (001)

Raul O. Freitas · Christoph F. Deneke · Ângelo Malachias · Gaspar Darin · Sérgio L. Morelhão

Received: 19 October 2012 / Accepted: 19 February 2013 / Published online: 10 March 2013

Abstract Friedel pairs are susceptible to symmetry breaking in crystals. Under resonant scattering conditions, non-centrosymmetric crystals can give rise to pairs of *hkl* and $\bar{h}\bar{k}\bar{l}$ reflections with different diffracted intensities, which are quantified as an anomalous signal of the structure. In bulk crystals, the shift in the anomalous signal through an absorption edge can be measured with good accuracy regardless the crystalline quality of the sample, leading to experimental values in agreement with theoretical ones. With the advance of nanotechnology and synchrotron sources, it has been possible to produce free-standing nanomembranes of semiconductor crystals, opening the opportunity of checking the measurability of anomalous signal in nanoscale materials. In this study, we describe a successful procedure to measure the anomalous signal in nanomembranes of GaAs (001) 15-nm thick with synchrotron radiation. Different membrane processing methods and diffraction geometries were tested, and major sources of instrumental inaccuracy were identified. Relevances of this type of measurements in nanotechnology as well as in basic science are discussed.

Keywords Bijvoet pairs · Free-standing nanomembranes · Single crystals · Synchrotron X-ray diffraction · Atomic resonance

Special Issue Editors: Juan Manuel Rojo, Vasileios Koutsos

This article is part of the topical collection on Nanostructured Materials 2012

R. O. Freitas
Brazilian Synchrotron Light Laboratory (LNLS), Campinas, Brazil

C. F. Deneke
Brazilian Nanotechnology National Laboratory (LNNano), Campinas, Brazil

C. F. Deneke
IFW Dresden, Dresden, Germany

Â. Malachias
Departamento de Física, Universidade Federal de Minas Gerais, Belo Horizonte, Brazil

G. Darin · S. L. Morelhão (✉)
Instituto de Física, Universidade de São Paulo, São Paulo, Brazil
e-mail: morelhao@if.usp.br

Introduction

Absorption spectroscopy is a very powerful technique to probe the local structure around atomic species in solids. Changes in the quantum levels due to chemical bonds and scattering potentials of neighboring atoms modulate the absorption probabilities, which can be observed by measuring the linear absorption coefficient as a function of X-ray photon energy E. By an energy conservation principle, known as "the optical theorem", the imaginary part $f''(E)$, of the resonant amplitude scattered by

an atom is related to its absorption cross-section $\sigma_a(E)$ according to (Lovesey 1996)

$$f''(E) = E\sigma_a(E)/4\pi r_e \hbar c = \sigma_a(E)/2r_e\lambda \quad (1)$$

where $r_e = 1.818 \times 10^{-15}$ m and λ is the selected wavelength. By using general properties of complex functions, it is also possible to obtain the real part $f'(E)$, of the atomic resonant amplitude, leading to the total scattering amplitude $f(q,E) = f_0(q) + f'(E) + if''(E)$ of an atom. Angular dependence with the direction of scattering is provided by $f_0(q)$, the atomic scattering amplitude, in electron units, without accounting effects of resonance and given as a function of diffraction vector modulus $q = 4\pi\sin(\theta)/\lambda$. The scattering angle 2θ regards the incident beam direction ($2\theta = 0$).

In crystals undergoing Bragg diffraction, complex atomic scattering factors are known to break Friedel's law for hkl and $\bar{h}\bar{k}\bar{l}$ reflections susceptible to the absence of symmetry center in the atomic structure (Giacovazzo 2002). Hence, the diffracted intensities I_{hkl} and $I_{\bar{h}\bar{k}\bar{l}}$ from such pairs of reflections are different when $f''(E) \neq 0$ for at least one atom in the structure. The anomalous signal

$$Q = \frac{I_{\bar{h}\bar{k}\bar{l}} - I_{hkl}}{I_{\bar{h}\bar{k}\bar{l}} + I_{hkl}} \quad (2)$$

is therefore a consequence of electronic transitions in atomic levels. For free atoms, transitions occur for the continuous quantum states of ejected photoelectrons, and the related amplitudes of resonance have been properly calculated and listed (Hubbell et al. 1975). Measurements of anomalous signals could be used, in principle, to probe variations in the quantum levels around an atom, exactly as in absorption spectroscopy. In practice, measuring absorption is much simpler than the anomalous signal in bulk materials. But, the same is not true for low-dimensional structures where X-ray absorption might be too weak to be detected. Probing small symmetry changes in nanocrystals under external forces is another example of situation where the anomalous signal measurements can be useful (Azimonte et al. 2010).

X-ray diffraction in nanoscale materials, such as in thin films and quantum wires and dots (Pietsch et al. 2004), is very accurately described on the basis of kinematical diffraction theory where the diffracted intensities are proportional to the squared modulus of the structure factors, i.e.

$$I_{hkl} \propto |F_{hkl}|^2 = \left| \sum_a C_a [f_0 + f' + if'']_a e^{2\pi i(hx_a + ky_a + lz_a)} \right|^2 \quad (3)$$

with index a running over all atoms of fractional coordinates (x_a, y_a, z_a) and occupation factor C_a in the average unit cell. This proportionality relationship allows composition analysis in nanostructures when comparing diffracted intensities at two or more energies close to the absorption edge of the element of interest, see for instance Malachias et al. (2012). The accuracy of such analysis depends on the given values of f' and f'', which are, in the best cases, experimental values from bulk crystals.

In this study, we investigate the feasibility of measuring anomalous signal from free-standing nanomembranes of GaAs, as well as the proportionality relationship stated in Eq. (3) as a function of energy. Since nanostructured devices are often grown on top of single crystals, anomalous signals and intensity behavior (as a functions E) in semiconductor substrates are also investigated experimentally and by dynamical diffraction simulation. Nanomembranes of GaAs (001) were prepared with distinct processing methods, and two different X-ray diffraction geometries were tested.

Kinematical and dynamical diffraction

Since diffraction intensities are proportional to $|F_{hkl}|^2$ in nanoscale materials where the kinematical approach is valid, it is straightforward to see from Eq. (2) that

$$Q = \frac{|F_{\bar{h}\bar{k}\bar{l}}|^2 - |F_{hkl}|^2}{|F_{\bar{h}\bar{k}\bar{l}}|^2 + |F_{hkl}|^2} \; . \quad (4)$$

In large perfect crystals, such as semiconductor substrates with a few hundred of microns thick, the diffraction phenomenon has to account for successive bounce of photons inside the crystal, which means that diffraction is dynamical and the intensities are not directly proportional to $|F_{hkl}|^2$. Nevertheless, the anomalous signal is only a function of the structure factors, exactly as given in Eq. (4). To demonstrate this fact, we have performed dynamical diffraction simulation in both thin and thick GaAs (001) crystals, Fig. 1.

Pairs of reflections providing the same Q value of a Friedel pair are known as Bijvoet pairs (Giacovazzo

2002). In III–V semiconductors, space group $F\bar{4}3m$, $hkl/\bar{h}\bar{k}l$ and $hkl/h\bar{k}\bar{l}$ are Bijvoet pairs that can be measured on the same side of a (001) crystal with just a 90° shift on its azimuth, e.g., rotation axis φ in Fig. 2b. In the kinematical regime of diffraction, Fig. 1a, the intensity reflectivity of one reflection increases while the other decreases when moving in energy from below to above the Ga absorption edge (at 10.368 keV). This is the expected behavior according to Eq. (3). On the other hand, in the dynamical regime of diffraction, one reflectivity maximum remains nearly constant while the other shows a drastic reduction, Fig. 1b. Although the reflectivity curves are not proportional to $|F_{hkl}|^2$, the relative difference between the simulated curves leads to the Q value predicted by Eq. (4). For instance, the areas under the reflectivity curves at $E = 10.4$ keV are $A_{111} = 149.4$ mrad and $A_{\bar{1}11} = 203.5$ mrad, providing $Q = (A_{\bar{1}11} - A_{111})/(A_{\bar{1}11} + A_{111}) = 0.153$, which is the same value obtained by using $|F_{111}| = 125.2$ and $|F_{\bar{1}\bar{1}\bar{1}}| = 146.1$ in Eq. (4). In this study, all theoretical values were obtained using scattering factors of free atoms (Prince 2006).

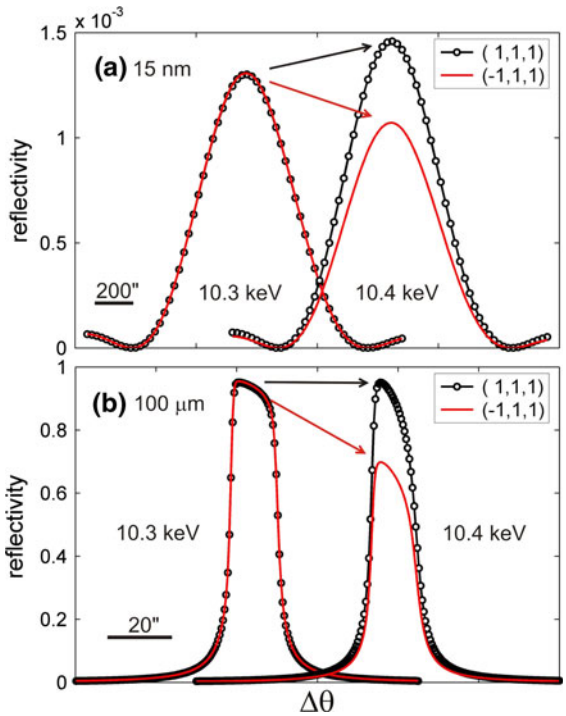

Fig. 1 Dynamical diffraction simulation for 111 and $\bar{1}11$ reflections in both thin and thick GaAs (001) crystals: **a** 15-nm and **b** 100-µm thick slab. The diffraction geometry is detailed in Section X-ray data acquisition, Fig. 2b. X-rays energies are indicated close to the simulated curves, which are displaced in the $\Delta\theta$ axis for clarity

Experimental

Sample preparation

The samples were grown by solid-source molecular beam epitaxy (MBE) using an Omicron III–V machine (IFW Dresden). Following a well-established growth procedure (Deneke et al. 2002), a 300-nm-thick $Al_{0.9}Ga_{0.1}As$ layer and a 15-nm GaAs top layer were deposited onto a GaAs (001) substrate. Layers deposition was monitored by reflective high energy electron diffraction, which showed a sticky diffraction pattern throughout the growth of the layers. After growth, free-standing membranes were produced as follows (Malachias et al. 2008; Rastelli et al. 2012).

In sample #1, Fig. 2a, a batch of rounded membranes, 100 µm in diameter and set apart by 200 µm, was defined by optical lithography and wet chemical etching using H_3PO_4 (85 vol%):H_2O_2 (35 vol%):H_2O (1:2.5:10). Without removing the resist on top of the membranes, the sample was etched with a HF (3 vol%) to attack the $Al_{0.9}Ga_{0.1}As$ layer and releases the membranes from the substrate (Deneke et al. 2002). As the membranes fall back to the original substrate, they could be transferred to a new host—in this case a Si (001) substrate—by spinning PMMA onto the host substrate and pressing the original sample onto it (Rastelli et al. 2012).

In sample #2, Fig. 2b, 1-µm-wide holes 10 µm apart were produced by optical lithography and chemical etching in HBr (48 vol%):$K_2Cr_2O_7$ (0.5 mol/l):CH_3COOH. After removal of the photoresist, a free-standing membrane was obtained by selective removal of the AlGaAs layer with HF (3 vol%). The membrane was transferred to a new GaAs (001) host substrate by fishing the free-floating membrane from the water surface.

X-ray data acquisition

X-ray diffraction experiments were carried out at diffraction station XRD2 of the Brazilian Synchrotron Light Laboratory (LNLS): bending magnetic

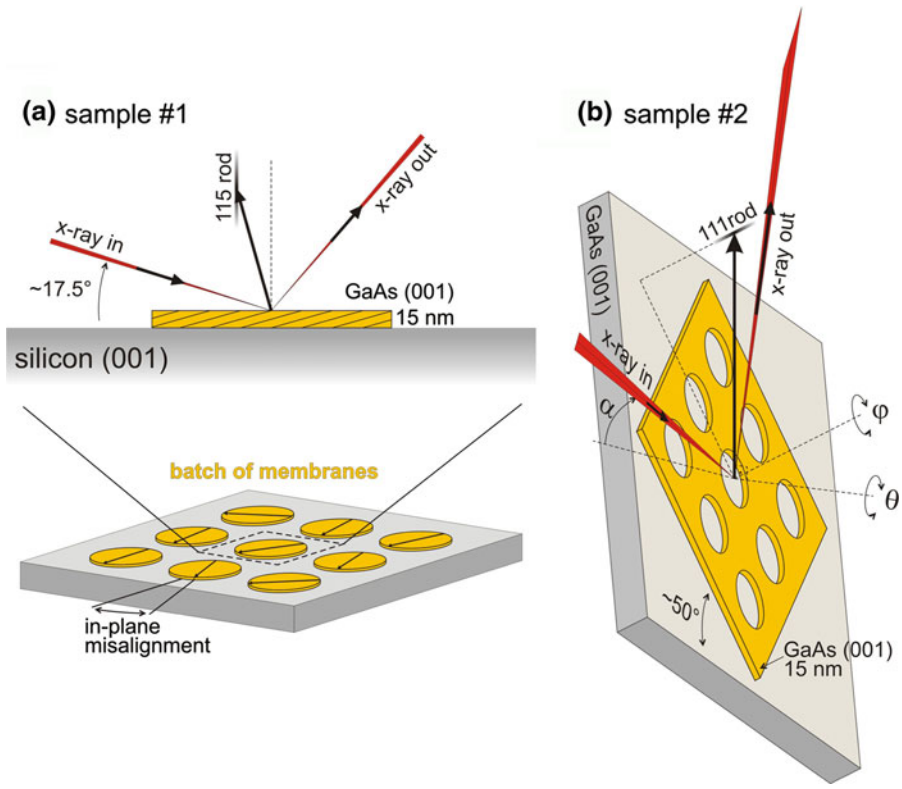

Fig. 2 Diffraction geometries of asymmetric reflections: **a** $115/\bar{1}15$, sample #1, batch of membranes on a silicon (001) substrate; **b** $111/\bar{1}11$, sample #2, a single membrane on a GaAs (001) substrate

beamline with focusing mirror and two-bounce Si (111) monochromator with a sagittal focusing second crystal. X-ray optics was in focused beam mode (sagittal crystal focused at the sample position, mirror focused at infinity), providing a vertical beam divergence of about 90 μrad (transversal coherence $\simeq 0.7$ μm) and an axial (horizontal) divergence of 10 mrad. Beam cross-section at sample position was 0.5×0.5 mm^2, and the diffraction plane is at the vertical position (σ polarization). Photon energies in the range from $E = 10.2$ to 10.55 keV were used with an accuracy better than 1 eV, although the energy resolution is about 5 eV (longitudinal coherence > 0.12 μm). Fluctuation in the incident beam intensity is monitored by measuring air scattering, which delivers a monitor signal. Two diffraction geometries have been employed. Asymmetric reflections such as 115 and 117 were measured with sample's surface normal direction in the diffraction plane, e.g., Fig. 2a, while 111 type of asymmetric reflections were set with the surface normal direction, rotation axis φ in Fig. 2b, at 35.264° from the horizontal direction. In all cases, diffraction intensities were corrected by the monitor signal, and the Q values determined by integrating the diffraction curves.

Results and discussion

A general preliminary test of $115/\bar{1}15$ and $117/\bar{1}17$ Bijvoet pairs have been carried out on a different bulk materials, on two wide pieces of a 0.5-mm-thick gallium antimonide substrate, GaSb (001). Average experimental and theoretical Q values were adjusted for the sake of comparison, showing a very good agreement within an accuracy of 10 %, Fig. 3.

Regarding the samples with nanomembranes. In sample #1, only the $115/\bar{1}15$ pair could be observed at the low incidence angle geometry, Fig. 2a. The wide axial divergence of the incident beam was crucial to enlarge the contribution of the ensemble of in-plane misaligned nanomembranes. These misalignments, not larger than 2°, were probably introduced during transfer to the host Si (001) substrate. Diffraction curves collected at energies of 10.3 and 10.4 keV for the nanomembranes in sample #1 are shown in Fig. 4.

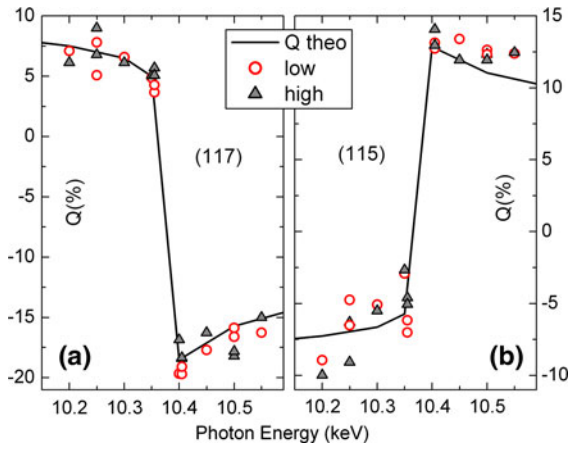

Fig. 3 Anomalous signal Q from **a** $117/\bar{1}17$ and **b** $115/\bar{1}15$ Bijvoet pairs in buck gallium antimonide, GaSb (001), crystals. Experimental values obtained at both low (*circles*) and high (*triangles*) incidence angles are compared to theoretical ones (*solid lines*)

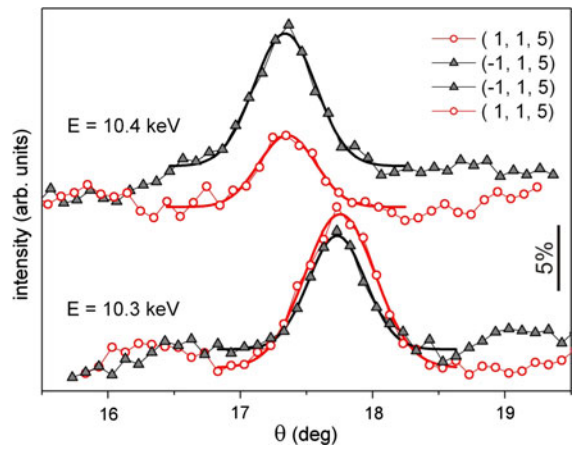

Fig. 4 Rocking curves of 115 and $\bar{1}15$ reflections in GaAs nanomembranes, sample #1. Gaussian fits (*solid lines*) are shown. *Curves* with different energies are displaced in the *vertical axis* for clarity. *Scale bar* stands for 5 % of intensity over the background of 10^5 counts/30 s

Peak intensities range from 5 to 10 % above the background noise of 10^5 counts/30 s due to nearby silicon substrate reflections, about 1.5° away. The area under the curves, above the background, were determined by Gaussian fit. Since the number of membranes illuminated by the X-ray footprint can change when rotating the sample to excite one reflection or the other, the areas were normalized by the one measured at the lower energy, and hence, $A_{115} = A_{\bar{1}15} = 1$ at $E = 10.3$ keV and $A_{115} = 0.42 \pm 0.04$ and $A_{\bar{1}15} = 1.27 \pm 0.02$ at $E = 10.4$ keV. The only accessible quantity is therefore the relative shift $\delta Q_e = 50 \pm 5$ % in the Q values from one energy to the other. The theoretical shift is $\delta Q_t = 27.7$ %, implying in a disagreement of 80 ± 20 % between experimental and theoretical values, see Fig. 5 (inset).

A much stronger signal/noise ratio was obtained from a single nanomembrane, sample #2, for the $111/\bar{1}11$ pair of reflections. A relative 50° in-plane rotation of the membrane lattice regarding the host GaAs (001) substrate allowed us to measure separately diffraction curves from both membrane and substrate lattices with the same diffraction geometry, Fig. 2b. As a function of energy, the determined Q values are compared to theoretical ones in Fig. 5. Except for the data point at the energy of 10.2 keV, the Q values from the membrane are just displaced by about + 2 % from the substrate ones. But, both membrane and substrate values provide nearly the same shift of $\delta Q_e = 14$ %,

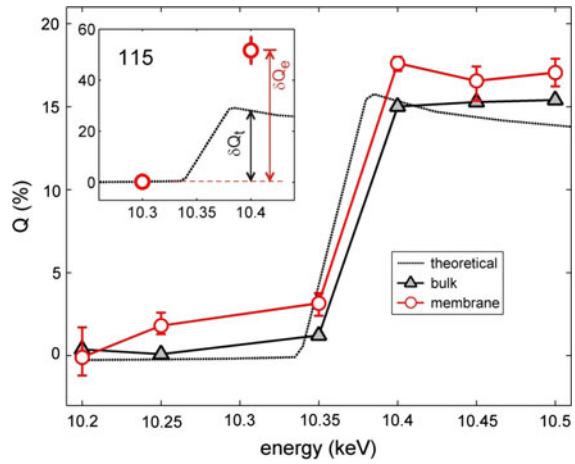

Fig. 5 Anomalous signal Q from $111/\bar{1}11$ reflections in both membrane and substrate of GaAs (001), sample #2. *Inset* theoretical (*dashed line*) and experimental (*circles*) Q values, as observed by $115/\bar{1}15$ reflections in a batch of nanomembranes, sample #1

slightly smaller than the theoretical one, $\delta Q_t = 15.5$ %, for scattering factors of free atoms.

Figure 6 shows the integrated diffraction curves plotted as a function of energy. For the membrane, the curve behavior is very similar to the expected one according to kinematical diffraction, Fig. 6a. The major disagreement is caused by an unexpected intensity drop of the $\bar{1}11$ reflection after the reference point. This is probably indicating that the beam position over the membrane has moved when

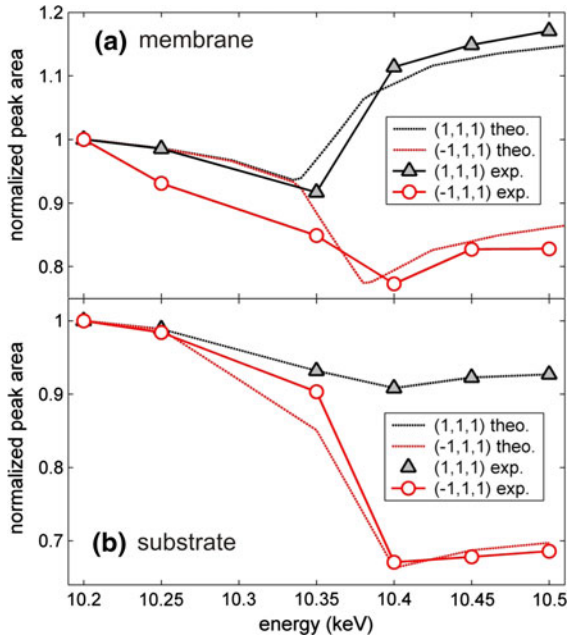

Fig. 6 Integrated diffraction curves as a function of energy: **a** nanomembrane and **b** substrate. Expected behavior (*dashed lines*) according to the **a** kinematical and **b** dynamical theories are shown. All quantities were normalized by their values at $E = 10.2$ keV. Further correction has been applied to substrate data as explained in the text

changing the energy from 10.2 to 10.25 keV. For the substrate, the strong intensity from its reflections was also sensitive to a systematic reduction of linear attenuation in air and windows of the beamline as the energy increases. Then, to compare the substrate data with the expected dynamical diffraction behavior, the experimental data were further normalized by the theoretical values of the 111 reflection. A very good match is thus obtained, Fig. 6b.

When the beam impinges the surface at $\alpha \simeq 6°$, Fig. 2b, the membrane thickness projection along the incident beam direction is 0.14 μm, which is of the same order of the longitudinal coherence length. Therefore, obtaining the same anomalous signal for membrane and substrate is a consistent result, demonstrating the feasibility of such measurements in free-standing nanostructures. On the other hand, the membrane thickness projection for 115 reflections, Fig. 2a, drops to 0.05 μm, something in between half and a third of the longitudinal coherence length. Although, the large discrepancy of the experimental data with theory obtained for the batch of membranes in sample #1 could be caused by either low signal/noise ratio or beam movement when changing the energy, or even by both, further confirmation is necessary. The optical theorem provides the correlation between the atomic absorption cross-section and the imaginary part of the forward scattering amplitudes, i.e., Eq. (1) applies to $\mathrm{Im}\{f(0,E)\}$. With no experimental evidence that the resonant amplitudes vary with the scattering angle, f' and f'' have been assumed to vary with energy only.

Since resonant amplitudes remain constant as a function of the diffraction vector, the relative contribution of the non-resonant amplitude, $f_0(q)$, decreases as the diffraction vector modulus increases. Therefore, larger anomalous signals are expected for reflections with higher indexes, e.g., $Q(10.4\ \mathrm{keV}) \simeq 41, 28$ and 15 % for the $117/\bar{1}17$, $115/\bar{1}15$ and $111/\bar{1}11$ pairs in bulk GaAs crystals, respectively. In nanostructures, measuring reflections with higher indexes can be very difficult due to the lower intensity of such reflections. Moreover, since experimental values of anomalous signals require measurements at different energies, the beam spot at the sample has to be kept stable within equivalent nanostructured areas when changing the energy. It adds an extra difficult in acquiring accurate values of anomalous signals. Current advances in designing synchrotron beamlines to provide coherent nanofocused X-ray beams of high flux can make routine analysis of anomalous signals from nanostructures possible in the near future. Scanning the Q signal with high resolution in energy may provide insights on how electronic levels in crystalline lattices of low dimensionality are susceptible to foreign chemical species at their surfaces. It is a different concept of absorption spectroscopy, which overlaps signals from amorphous and crystalline regions present in the samples.

Conclusions

In this study, we demonstrate the feasibility of measuring anomalous signals from free-standing one-dimensional nanostructures, 15-nm-thick GaAs membranes, arranged in different configurations. In acquiring the collective signal from several membranes, their relative misalignments have restricted the diffraction geometry to one that could use the axial divergence for increasing the signal. Nearby reflections of the host substrate were essential to locate the weak reflections of the membranes, although they

raise the background noise compromising accuracy in determining the signal values. A large discrepancy between experimental and theoretical values was found, which requires further investigation with more appropriate instrumentation and optimized samples: high flux, focused, and stable X-ray beams, as well as membranes with large flat areas.

For analyzing a single membrane, suitable diffraction geometry could be employed. It has enlarged the diffraction volume, boosting the signal accuracy to the same one obtained from bulk materials. Stable beam spots when scanning the X-ray energy is a crucial requirement for future exploitation of anomalous signals in nanostructured devices.

Acknowledgments We acknowledge the funding agency for research of the São Paulo State FAPESP (Proc. No. 2012/15858-8), the National agency CNPq (Proc. No. 304247/2009-0) and support of the Brazilian synchrotron. Thanks are also due to M.H. de Oliveira Piazetta and A.L. Gobbi from LMF-LNNano for lithography in microfabrication of the membranes.

References

Azimonte C, Granado E, Terashita H, Park S, Cheong S-W (2010) Polar atomic displacements in multiferroics observed via anomalous X-ray diffraction. Phys Rev B 81: 12103. doi:10.1103/PhysRevB.81.012103

Deneke C, Muller C, Jin-Phillipp NY, Schmidt OG (2002) Diameter scalability of rolled-up In(Ga)As/GaAs nanotubes. Semicond Sci Technol 17:1278–1281. doi:10.1088/0268-1242/17/12/312

Giacovazzo C (ed) (2002) Fundamentals of crystallography, 2nd edn. Oxford University Press, Oxford

Hubbell JH, Veigele WmJ, Briggs EA, Brown RT, Cromer DT, Howerton RJ (1975) Atomic form factors, incoherent scattering functions, and photon scattering cross sections. J Phys Chem Ref Data 4:471–538. doi:10.1063/1.555523

Lovesey SW, Collins SP (1996) X-ray scattering and absorption by magnetic materials. Clarendon press, Oxford

Malachias A, Mei YF, Annabattula RK, Deneke C, Onck PR, Schmidt OG (2008) Wrinkled-up nanochannel networks: long-range ordering, scalability, and X-ray investigation. ACS Nano 2:1715–1721. doi:10.1021/nn800308p

Malachias A, Freitas R, Morelhão S, Magalhães-Paniago R, Kycia S, Medeiros-Ribeiro G (2012) X-ray diffraction methods for studying strain and composition in epitaxial nanostructured systems. In: Haight R, Ross FM, Hannon JB, Feldman LC (eds) Handbook of instrumentation and techniques for semiconductor nanostructure characterization. World Scientific, Hackensack, pp 256–324

Pietsch U, Holý V, Baumbach T (2004) High-resolution X-ray scattering: from thin films to lateral nanostructures. Springer, New York

Prince E (ed) (2006) International tables for crystallography, volume C: mathematical, physical and chemical tables. Wiley, New York, pp 554–590

Rastelli A, Ding F, Plumhof JD, Kumar S, Trotta R, Deneke C, Malachias A, Atkinson P, Zallo E, Zander T, Herklotz A, Singh R, Krápek V, Schröter JR, Kiravittaya S, Benyoucef M, Hafenbrak R, Jöns KD, Thurmer DJ, Grimm D, Bester G, Dörr K, Michler P, Schmidt OG (2012) Controlling quantum dot emission by integration of semiconductor nanomembranes onto piezoelectric actuators. Phys Status Solidi (b) 249: 687–696. doi:10.1002/pssb.201100775